Allylic alcohol synthesis by gas-phase hydrogen transfer reduction of unsaturated ketones

J.I. Di Cosimo*, A. Acosta, C.R. Apesteguía

Catalysis Science and Engineering Research Group (GICIC), Instituto de Investigaciones en Catálisis y Petroquímica-INCAPE-(UNL-CONICET), Santiago del Estero 2654, 3000 Santa Fe, Argentina

Abstract

The gas-phase hydrogen transfer reduction (HTR) of mesityl oxide (MO) with 2-propanol to selectively obtain allylic alcohols was studied on MgO. MO was converted directly to 4-methyl-3-penten-2ol (UOL_1) or isomerised to *iso*-mesityl oxide (*i*-MO), which consecutively formed 4-methyl-4-penten-2ol (UOL_2). Significant amounts of methyl isobutyl carbinol (MIBC) were also formed by the simultaneous reduction of C=C and C=O groups of MO. The effect of reaction conditions on catalyst activity and selectivity was determined in order to improve total UOL yield that was about 28% under standard reaction conditions ($T = 523$ K, 2-propanol/MO = 5, $W/F_{MO}^0 = 15$ g h/mol). Total UOL yield increased continuously with contact time up to 42% but when the 2-propanol/MO ratio was varied, UOL yield reached a maximum at a reactant ratio of about 4. UOL_2 yield markedly increased with temperature at expenses of MIBC. The increase of temperature also improved the catalyst stability because suppressed formation of coke intermediates. Regarding the effect of the hydrogen donor, higher total UOL yields were obtained by using secondary alcohols, such as 2-propanol and 2-butanol, than primary (1-propanol) or secondary aryl (1-penylethanol) alcohols.
© 2005 Elsevier B.V. All rights reserved.

Keywords: Hydrogen transfer; Basic catalysis; α,β-Unsaturated ketone; Reduction; Chemoselectivity

1. Introduction

The selective synthesis of primary and secondary unsaturated alcohols is an important process for pharmaceutical, fragrance and food flavoring industries. Among unsaturated alcohols, those derived from allylic ketones (secondary alcohols) are in particular, valuable products used in polymer industry. Synthesis of allylic alcohols via allylic ketone reduction on noble metals by conventional hydrogenation that uses high-pressure H_2 in multiphase batch reactors is hardly achieved because of the higher reactivity of the C=C bond compared with that of C=O group [1] and because the substituent at the carbonyl hinders saturation of the C=O bond [2]. In addition, isomerization of the unsaturated alcohol formed to the corresponding saturated ketone is usually an

unavoidable side reaction on metallic catalysts that affects allylic alcohol yield [3]. Nevertheless, a paper by von Arx et al. [4] and more recently another by Milone et al. [5] report significant unsaturated alcohol yields for the liquid-phase reduction of ketoisophorone on Pd/Al_2O_3 and several unsaturated ketones on Au/Fe_2O_3, respectively. These two contributions are so far the only successful attempts of the use of molecular hydrogen and metallic catalysts for selective hydrogenation of unsaturated ketones toward unsaturated alcohols in liquid phase. Still, there is no report in the literature dealing with gas-phase hydrogenation of unsaturated ketones on metallic catalysts.

Hydrogen transfer reduction (HTR) reactions from an alcohol to a carbonyl compound have been successfully explored for C=O bond reduction of α,β-unsaturated aldehydes and may provide an alternative route for selective reduction of α,β-unsaturated ketones in spite of the fact that the substituent to the C=O bond makes the reduction of ketones more
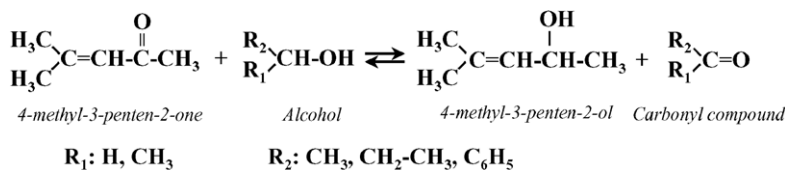
difficult [6]. HTR is a redox reaction in which the reactant carbonyl compound (the oxidant) is contacted in gas or liquid phase with a hydrogen donor (the reductant, usually a secondary alcohol), thereby, avoiding the use of pressurized H_2.
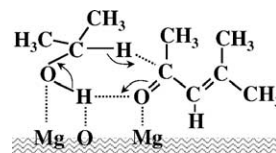
Heterogeneously catalyzed HTR of unsaturated carbonyl compounds are believed to occur on metal oxides, zeolites or mesoporous materials via a Meerwein–Ponndorf–Verley (MPV) mechanism, which involves the selective reduction of the C=O bond, preserving the other reducible functional group, the C=C bond [7–9]. The chemoselectivity of this process arises from the fact that the mechanism proceeds without formation of molecular hydrogen by hydride transfer from the alcohol via a cyclic six-membered intermediate, comparable to that postulated for the homogeneous MPV reaction, in which both reactants are coordinated to a metal cation [10].

Very few attempts can be found in the literature regarding the liquid-phase synthesis of secondary allylic alcohols by HTR of unsaturated cyclic, aryl or allylic ketones [8,9,11–13] and even fewer in the gas phase [7,14–16]. Nevertheless, the development of competitive gas-phase continuous flow processes, as an alternative to the liquid-phase batch process would present high technological impact. But the use of higher reaction temperatures in the gas-phase process enables different reaction pathways to be followed by the catalytic reaction giving rise therefore, to selectivity problems. Efforts devoted to elucidate the reaction pathways involved and to study the operational conditions for improving the allylic alcohol yield are still needed.

In a previous paper [17], we studied the gas-phase HTR of an α,β-unsaturated ketone, mesityl oxide (4-methyl-3-penten-2-one) with 2-propanol toward the unsaturated alcohol (4-methyl-3-penten-2-ol), Eq. (1), on acid–base and metal/acid–base catalysts, specifically on MgO, $MgAl_{0.33}O_x$ and $Cu_{0.05}MgAl_{0.65}O_x$ oxides. We found that $MgAl_{0.33}O_x$ and $Cu_{0.05}MgAl_{0.65}O_x$ catalysts, selectively reduce the C=C bond, thereby,

Scheme 1. HTR reaction of mesityl oxide with 2-propanol on MgO. Surface reaction intermediate for allylic alcohol formation by MPV mechanism.

surface reaction intermediate as shown in Scheme 1. Contrarily, more electronegative cations such as Al^{3+} as well as Cu^0 metallic sites adsorb 2-propanol dissociatively forming surface hydrogen fragments that selectively reduce the C=C bond by a mechanism different from that of the MPV reaction.

In this paper, and based on previous findings, we continue our investigations on the gas-phase HTR of mesityl oxide on MgO. Our goal was to determine the optimum conditions for maximum allylic alcohol yield. Because of competitive reactions might take place in the gas-phase, we investigated the reaction pathways leading to allylic alcohol and other compounds by varying the contact time when reactants are fed to the reactor together or separately. We also carried out a systematic study of the effect of the different operational variables on the catalyzed process leading to allylic alcohol formation as well as on the thermodynamics of this reaction and on catalyst deactivation. Thus, we discussed the effect of reaction temperature, alcohol/ketone ratio and type of hydrogen donor.

2. Experimental

2.1. Catalyst synthesis

High surface area pure MgO was prepared by hydration with distilled water at room temperature of commercial

(1)

shifting the reaction pathway toward the saturated ketone. In contrast, MgO promotes efficiently the HTR of mesityl oxide toward the unsaturated alcohol. We interpreted those results in terms of the role played by the different surface species (acid–base or metallic) in the coordination of the carbonyl group. Specifically, the distinctive catalytic behavior of MgO was attributed to the weak Lewis acid-strong base character provided by the Mg^{2+}–O^{2-} pairs, that defines the particular surface adsorption modes of both reactants: mesityl oxide interacts via the C=O bond with a weak Lewis acid Mg^{2+} cation and 2-propanol adsorbs non-dissociatively on a vicinal Mg^{2+}–O^{2-} pair, giving rise to a

MgO (Carlo Erba, 99%, 0.2% Na, 0.005% Fe, $27\,m^2/g$) and further decomposition in N_2 at 773 K. Details are given elsewhere [18].

2.2. Catalyst characterization

BET surface area (S_g) was measured by N_2 physisorption at its boiling point using a Quantachrome Nova-1000 sorptometer.

The total CO_2 adsorption site density and binding energies were obtained from temperature-programmed des-

orption (TPD) of CO_2 preadsorbed at room temperature. Sample (150 mg) was pretreated in N_2 at 773 K for 1 h and then exposed to a flow of 100 cm^3/min of 3.09% CO_2/N_2 at room temperature until saturation coverage was reached. Weakly adsorbed CO_2 was removed by flowing N_2 and then the temperature was increased to 773 K at 10 K/min. The evolved CO_2 was converted to methane on a methanation catalyst (Ni/Kieselghur) operating at 673 K and monitored using a flame ionization detector. The structure of CO_2 chemisorbed on MgO was determined by infrared spectroscopy (IR). Data were obtained using a Shimadzu FTIR-8101M spectrophotometer. Details are given elsewhere [19].

2.3. Catalytic testing

Catalytic tests were conducted at typically 523 K and atmospheric pressure in a fixed bed reactor. Sample sieved at 0.35–0.42 mm was pretreated in N_2 at 773 K for 1 h before reaction in order to remove adsorbed H_2O and CO_2.

The reactants, mesityl oxide, MO (Acros 99%, isomer mixture of mesityl oxide/*iso*-mesityl oxide (*i*-MO) = 91/9), and 2-propanol, 2P (Merck, ACS, 99.5%), were introduced as a mixture with the proper molar composition via a syringe pump and vaporized into flowing N_2 to give a N_2/2-propanol = 12 (molar ratio). Reaction products were analyzed by on-line gas chromatography in a Varian Star 3400 CX chromatograph equipped with a flame ionization detector and a 0.2% Carbowax 1500/80–100 Carbopack C column. Main reaction products from MO conversion were identified as the two unsaturated alcohol isomers (UOL$_1$, 4-methyl-3-penten-2ol and UOL$_2$, 4-methyl-4-penten-2ol), *iso*-mesityl oxide, methyl isobutyl ketone (MIBK) and methyl isobutyl carbinol (MIBC). At high MO conversion levels, C$_9$ oxygenates such as phorones were also obtained. The total C$_9$ aldol condensation products are identified in the text as AC. Acetone (DMK) was produced by 2P oxidation in HTR reaction, Eq. (1). Small amounts of propylene were formed by 2P dehydration.

Some experiments were carried out with 1-propanol (Merck, 99.5%), 1-phenylethanol (Aldrich, 98%) and 2-butanol (Merck, 99%) as hydrogen donors; 1-propionaldehyde, acetophenone and methyl ethyl ketone, were the alcohol oxidation products, respectively, according to Eq. (1).

Selectivities (S_i, carbon atoms of product i/carbon atoms of MO reacted) and yields (η_i, carbon atoms of product i/carbon atoms of MO fed) were calculated as $S_i = \frac{F_i N_i}{\sum F_i N_i}$ and $\eta_i = \frac{F_i N_i}{6 F_{MO}^0}$, where F_i is the molar flow of a product i formed from MO; N_i, the number of carbon atoms in product i; and F_{MO}^0 is the molar flow of MO in the feed. Due to catalyst deactivation, the catalytic results reported here were calculated by extrapolation of the reactant and product concentration curves to zero time on stream. Then, X, S, and η represent conversion, selectivity, and yield at $t = 0$, respectively.

3. Results and discussion

3.1. Characterization

BET surface area of our MgO was 136 m^2/g. The nature of chemisorbed CO_2 species and a measure of the base site density were obtained by combining TPD and infrared measurements of CO_2 preadsorbed at room temperature. In previous work, we have extensively characterized by these techniques MgO samples prepared similarly to that used in this work [19].

The total amount of desorbed CO_2 measured by integration of TPD curve was 5.6 μmol/m^2. The complex TPD profile (not shown) reflected the presence of several types of adsorbed CO_2 and, thereby, suggests that the surface of MgO is nonuniform and contains surface base sites (oxygen anions) of different chemical nature. To confirm this, IR spectra of CO_2 adsorbed at room temperature were taken after sequential evacuation at increasing temperatures [19]. We identified three adsorption species which apparently reflect three surface base sites of different chemical nature and binding energies: unidentate and bidentate carbonates and bicarbonate [20]. Based on the IR characterization, the TPD profile was deconvoluted in three desorption bands: a low-temperature (L-peak) at 370 K, assigned to bicarbonates formed on weak Brönsted OH groups; a middle-temperature (M-peak) at 470 K attributed to bidentate carbonates desorbed from acid–base sites such as Mg^{2+}–O^{2-} pairs and a high-temperature peak (H-peak) at 540 K resulting from unidentate carbonates released from strongly basic low-coordination oxygen anions. The M-peak and H-peak are dominant on MgO, representing 47% and 40%, respectively, of the total evolved CO_2.

We have also determined before by combining NH_3 TPD [19] and FTIR of pyridine, the acidic properties of MgO. The low total density of acid sites (0.12 μmol/m^2) measured by NH_3 TPD and the fact that pyridine mostly adsorbed on Mg^{2+} Lewis acid cations is completely removed by evacuation at 373 K, reflect the poor acidic features of this material.

The presence on the MgO surface of a high concentration of vicinal Mg^{2+}–O^{2-} sites, in which the oxygen anion is a medium-strength base species as determined by CO_2 TPD and the Mg^{2+} cations are weakly acidic, makes MgO an attractive material for HTR since as it was previously explained [17], the reaction proceeds on metal-oxygen sites (Scheme 1) with that kind of acid–base properties.

3.2. Reaction pathways for individual reactants

Initially, and with the purpose of elucidating reaction pathways from each individual reactant, several catalytic experiments were carried out on MgO feeding the oxidant (MO) and the reductant (2P) separately.

Fig. 1 shows product yields and MO conversions at zero time on stream as a function of contact time ($W/F_{MO}^0 = 4$–35 g cat h/mol MO) obtained when only MO vaporized in
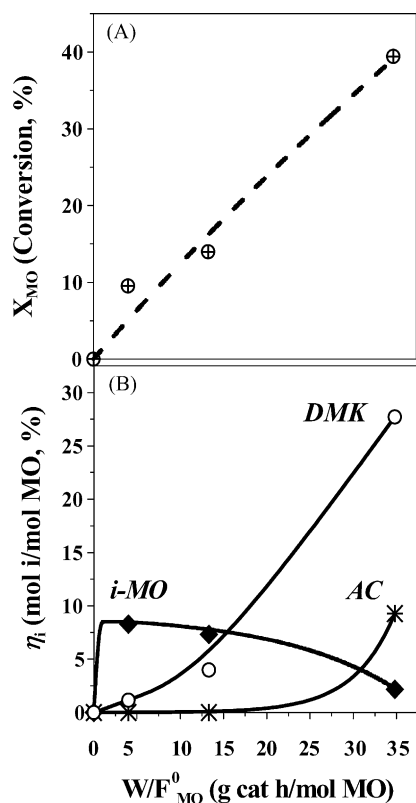
Fig. 1. Effect of contact time on gas-phase MO reactions ($T = 523$ K, $P_T = 100$ kPa, $N_2/MO = 99.8/1.5$, kPa): (A) MO conversion; (B) product yields.

Fig. 2. Effect of contact time on gas-phase 2P reactions ($T = 523$ K, $P_T = 100$ kPa, $N_2/2P = 93.5/7.8$, kPa): (A) 2P conversion; (B) product yields.

N_2 ($N_2/MO = 99.5/1.5$, kPa) is supplied in the feed. MO conversions (X_{MO}) of up to 40% were obtained within the contact time range studied.

At low contact times, double bond isomerization of MO was the main reaction leading to i-MO as a primary product. Similarly to isomerization of olefins on basic oxides, this reaction proceeds via carbanion intermediates [21]. Mobile surface protons generated in the isomerization reaction [17] seem unable to incorporate to the C=O bond of MO since we do not detect unsaturated alcohols among the products. At high contact times, secondary reactions took place with formation of DMK probably by a retroaldolization reaction (provided traces of water are present) and phorones (C_9 unsaturated ketones) by aldol condensation of MO with DMK (AC products). As expected, formation of products by reduction of the C=O or C=C bond of MO was not observed since there is no hydrogen donor reactant in the feed.

Similarly to the experiments with pure MO, pure 2P vaporized in N_2 ($N_2/2P = 93.2/7.8$, kPa) was contacted with MgO at different contact times ($W/F_{2p}^0 = 3$–85 g cat h/mol 2P). Results are shown in Fig. 2. MgO transformed 2P with conversions (X_{2P}) lower than 20% under these conditions. The main reaction was the 2P conversion to DMK + H_2 (alcohol dehydrogenation reaction), which is consistent with previous results showing that decomposition of a secondary alcohol to the corresponding ketone and molecular hydrogen is a reac-
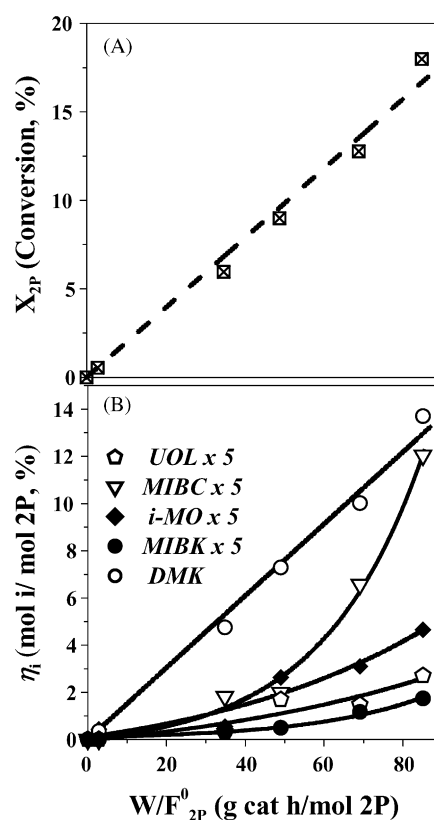
tion typically promoted by basic oxides [22]. Selectivities to DMK were in the range of 65–85%, in agreement with previous results showing that the competitive pathways leading to dehydration products, propylene (C_3=) and di-isopropyl ether are not favored on MgO catalysts [23]. The local slopes of the curves representing product yields as a function of contact time give the rate of formation of each product at a specific reactant conversion and residence time. Thus, the nonzero initial slope of the DMK curve in Fig. 2B is consistent with direct formation from 2-propanol.

DMK formed during the reaction is probably converted to MO by self-condensation. Although MO was not detected among the reaction products, the presence of i-MO, UOL, MIBK, and MIBC strongly suggests the fast and consecutive reduction of MO toward MIBC, UOL and MIBK as well as MO isomerization to i-MO. The zero initial slope of the i-MO curve in Fig. 2B supports consecutive formation from MO. In a similar way, MIBC and MIBK formed from MO or i-MO. Nevertheless, it has to be noted here that η_{MIBC} increased with contact time markedly more rapidly than η_{UOL} or η_{MIBK}, and that UOL and MIBK yield curves did not reach any maximum. These results suggest that MIBC is mainly formed directly by simultaneous reduction of C=C and C=O bonds of MO (or i-MO) and not via consecutive reactions from UOL or MIBK. The direct reduction of MO to MIBC is probably promoted by the presence of surface hydrogen frag-
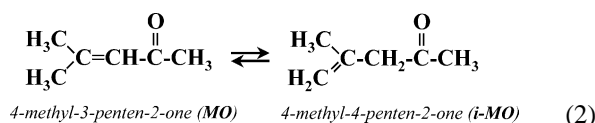
ments formed by dehydrogenation of 2P to DMK. In fact, in a previous paper [17], we studied the 2P conversion reactions on MgO and concluded that reduction of the C=C double bond of MO cannot be achieved without participation of surface hydrogen fragments from 2P dehydrogenation.

In summary, results in Fig. 2 show that HTR reactions occur on MgO when the reactant is pure 2-propanol provided that the conversion level is sufficiently high to allow formation of mesityl oxide by aldol condensation which behaves as a potential hydrogen acceptor in consecutive reactions.
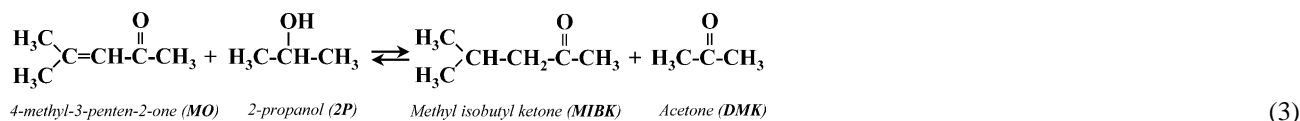
3.3. Effect of contact time

When both reactants (MO and 2P) are co-fed to the reactor, in addition to Eq. (1) several parallel or consecutive reactions can take place, such as:
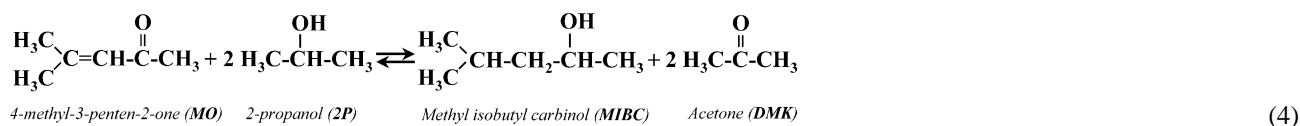
(i) MO double bond isomerization Eq. (2),

$$\begin{array}{c}H_3C\\H_3C\end{array}\!\!\!>\!\!C\!=\!CH\!-\!\overset{\overset{\displaystyle O}{\|}}{C}\!-\!CH_3 \;\rightleftharpoons\; \begin{array}{c}H_3C\\H_2C\end{array}\!\!\!>\!\!C\!-\!CH_2\!-\!\overset{\overset{\displaystyle O}{\|}}{C}\!-\!CH_3$$

*4-methyl-3-penten-2-one (**MO**)*   *4-methyl-4-penten-2-one (**i-MO**)*   (2)

(ii) Selective C=C bond reduction of MO or *i*-MO to MIBK, Eq. (3), which presents the same stoichiometry as Eq. (1):

$$\begin{array}{c}H_3C\\H_3C\end{array}\!\!\!>\!\!C\!=\!CH\!-\!\overset{\overset{\displaystyle O}{\|}}{C}\!-\!CH_3 + H_3C\!-\!\overset{\overset{\displaystyle OH}{|}}{C}H\!-\!CH_3 \;\rightleftharpoons\; \begin{array}{c}H_3C\\H_3C\end{array}\!\!\!>\!\!CH\!-\!CH_2\!-\!\overset{\overset{\displaystyle O}{\|}}{C}\!-\!CH_3 + H_3C\!-\!\overset{\overset{\displaystyle O}{\|}}{C}\!-\!CH_3$$

*4-methyl-3-penten-2-one (**MO**)*   *2-propanol (**2P**)*   *Methyl isobutyl ketone (**MIBK**)*   *Acetone (**DMK**)*

(3)

(iii) Simultaneous C=C and C=O bond reduction of MO or *i*-MO to MIBC, Eq. (4):

$$\begin{array}{c}H_3C\\H_3C\end{array}\!\!\!>\!\!C\!=\!CH\!-\!\overset{\overset{\displaystyle O}{\|}}{C}\!-\!CH_3 + 2\,H_3C\!-\!\overset{\overset{\displaystyle OH}{|}}{C}H\!-\!CH_3 \;\rightleftharpoons\; \begin{array}{c}H_3C\\H_3C\end{array}\!\!\!>\!\!CH\!-\!CH_2\!-\!\overset{\overset{\displaystyle OH}{|}}{C}H\!-\!CH_3 + 2\,H_3C\!-\!\overset{\overset{\displaystyle O}{\|}}{C}\!-\!CH_3$$

*4-methyl-3-penten-2-one (**MO**)*   *2-propanol (**2P**)*   *Methyl isobutyl carbinol (**MIBC**)*   *Acetone (**DMK**)*

(4)

(iv) Aldol condensation reactions between C_6 carbonyl compounds and DMK toward C_9 compounds.

The effect of contact time (W/F_{MO}^0 and W/F_{2p}^0) on the activity and product distribution was investigated by co-feeding both reactants (2P and MO) to the reactor with a 2P/MO = 5 (molar ratio) at 523 K. Contact times were varied in a wide range (W/F_{MO}^0 = 2.0–42.0 g cat h/mol MO; W/F_{2p}^0 = 0.5–8.4 g cat h/mol 2P). Results are shown in Fig. 3.

Thermodynamic calculations for Eq. (1) using additivity rules [24] for 2P as a hydrogen donor, Fig. 4, predict a MO equilibrium conversion of 80% at 523 K and 2P/MO = 5. For Eq. (1) taking place with 100% selectivity, the expected X_{MO}/X_{2P} conversion ratio should be 5 for a 2P/MO = 5 reactant composition. However, experimental results obtained at 523 K and 2P/MO = 5 (Fig. 3A) show that for a contact time of 42.0 g h/mol MO, the MO conversion and X_{MO}/X_{2P} ratio are 87% and 5.8, respectively, which reflects the presence of the additional reactions described above.

A comparative inspection of Figs. 1–3 clearly indicates that because hydrogen transfer reactions between MO and 2P take place, X_{MO} and X_{2P} are dramatically higher when both reactants are supplied together than separately. The initial MO conversion rate (r_{MO}^0) calculated from Fig. 3A is 711 μmol/h m² for a 2P/MO = 5 reactant composition whereas that from Fig. 1 for pure mesityl oxide in the feed is as low as 95 μmol/h m². This activity effect is even more pronounced for 2P since the initial 2P conversion rate (r_{2p}^0) calculated from Fig. 3A is 992 μmol/h m² in contrast to 14 μmol/h m² calculated from Fig. 2 for pure 2-propanol in the feed.

Irrespective of contact time, 2P dehydration products (propylene) were formed only in trace amounts, thereby, confirming that 2P participates essentially in hydrogen transfer reactions giving DMK. Fig. 3B shows the product yields for MO reactions as a function of contact time. Total UOL yield increased with W/F_{MO}^0 up to about 42% without reaching any maximum, thereby, suggesting that UOL does not participate significantly in consecutive reactions on MgO. This result differs from what is usually observed in liquid-phase HTR of ketones on noble metal catalysts, on which the allylic alcohol is rapidly isomerised to the saturated ketone [3] or further hydrogenated to the saturated alcohol [25].

Both UOL isomers, UOL_1 and UOL_2, formed fast and directly from MO and *i*-MO, respectively, as indicated by its non-zero initial slope in Fig. 3C. The isomerization compound, *i*-MO, is a primary product of mesityl oxide reactions. But *i*-MO is already present in a composition of 1.4% in the liquid reactant feed (see Section 2.3 above), what explains the non-zero initial slope for UOL_2 in Fig. 3C. A UOL_1/UOL_2 = 3 equilibrium molar ratio is predicted from our thermodynamic calculations at 523 K for isomerization of UOL_1 into UOL_2. Thus, the $UOL_1/UOL_2 < 3$ ratio measured in Fig. 3C at low contact times, suggests that UOL_2 forms directly from *i*-MO at low MO conversions. The fact that η_{UOL2} decreases at high contact times following $\eta_{i\text{-}MO}$ (Fig. 3B), indicates that also at high MO conversions UOL_2 comes mainly from reduction of *i*-MO rather than from isomerization of UOL_1.

MIBK yields of less than 1% were measured regardless of the conversion level, thereby confirming that selective reduc-
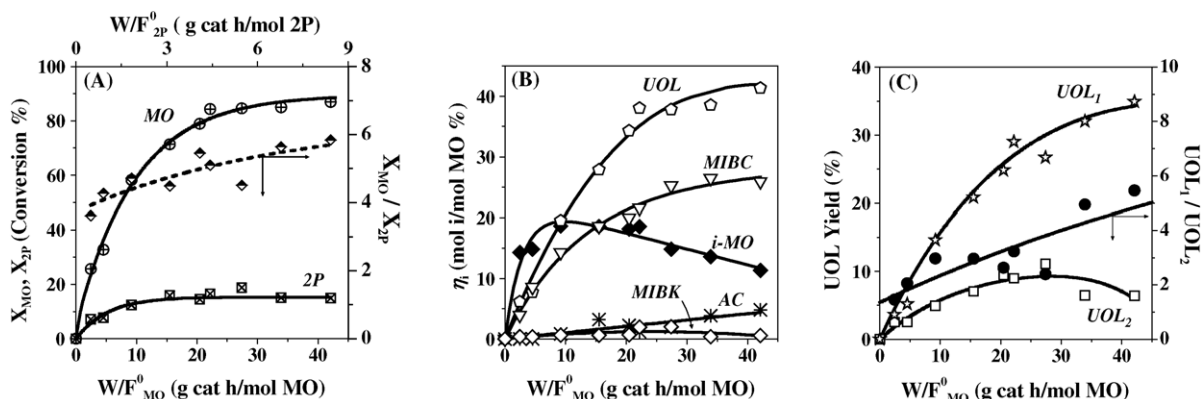
Fig. 3. Effect of contact time on gas-phase HTR of MO with 2P ($T = 523$ K, $P_T = 100$ kPa, $N_2/2P/MO = 93.4/6.6/1.3$, kPa): (A) reactant conversions; (B) product yields; (C) yield of UOL isomers.

tion of the C=C bond of mesityl oxide is unlikely on MgO. The MIBC curve in Fig. 3B is consistent with direct formation from MO at low conversions but also from *i*-MO or to a lesser extend from UOL at high contact times. Finally, the initial zero slope for AC product formation reveals that aldol condensation compounds are formed in consecutive pathways.

Results of Figs. 1–3 allow us to postulate the reaction kinetic network for HTR reactions on MgO depicted in Scheme 2, where the line width indicates the relative relevance of each reaction. MO is isomerised to *i*-MO and both isomers are reduced at high rates by 2-propanol to the corresponding allylic alcohols. MgO efficiently catalyzes UOL formation because it contains weak acid-strong base Mg^{2+}–O^{2-} pair sites that promote formation of the 6-atom cyclic intermediate needed in Meerwein–Ponndorf–Verley mechanism (Scheme 1) for preferentially transferring hydrogen from the 2-propanol donor molecule to the C=O bond of mesityl oxide [17]. In contrast, formation of MIBK is negligible because selective reduction of the C=C bond of mesityl oxide isomers does not take place on MgO. MO and *i*-MO are also transformed directly to MIBC at significant rates. In a

previous paper [17], we proposed that the unselective reduction of MO to MIBC on MgO occurs by a simultaneous di-π adsorption mode of both C=C and C=O bonds or by "on top" combined with $\pi_{C=C}$ adsorption modes on the Mg^{2+} cations. However, reduction of the C=C bond is not achieved via direct hydrogen transfer from 2P as in the MPV mechanism but from the surface H fragments provided by dehydrogenation of 2P to DMK as discussed above for interpreting the results in Fig. 2.

3.4. Effect of 2P/MO reactant ratio

De Graauw et al. [6] reported that the oxidant equilibrium conversion may be enhanced by using higher reductant/oxidant ratios or stronger reductants. In agreement with these researchers, thermodynamic calculations for Eq. (1) presented in Fig. 4 anticipate a positive effect of increasing the 2P/MO ratio on MO equilibrium conversion. Similar calculations for the HTR of MO toward MIBK or MIBC, Eq. (3) or (4), also predict that the higher the 2P/MO ratio in the feed, the higher the MO equilibrium conversion. Obviously,
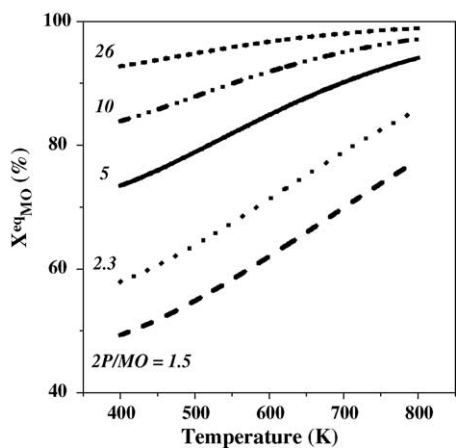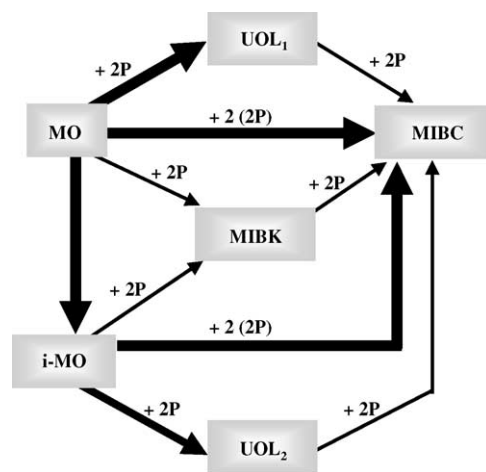

Fig. 4. MO equilibrium conversion for allylic alcohol formation by HTR of MO with 2P according to Eq. (1).

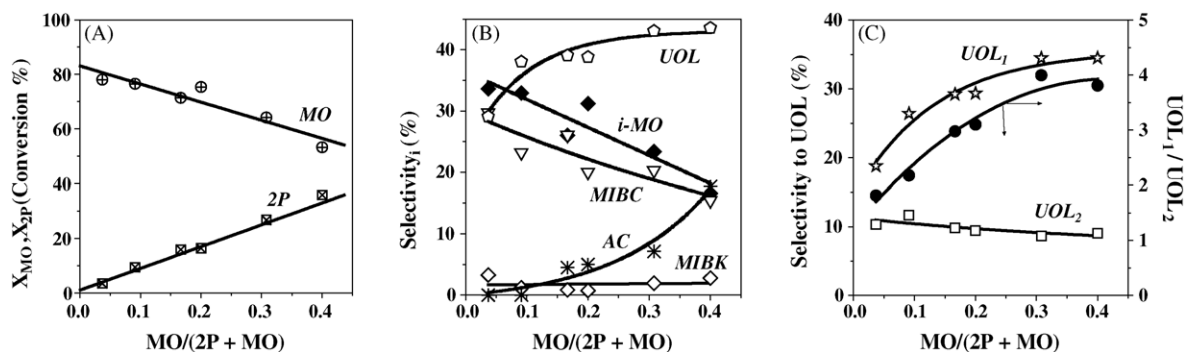Scheme 2. Reaction kinetic network for the HTR of mesityl oxide with 2-propanol on MgO.

Fig. 5. Effect of feed composition on gas-phase HTR of MO with 2P [$T = 523$ K, $P_T = 100$ kPa, $W/F_{MO}^0 = 15$ g h/mol MO, $P_{2p}^0 = 6.5$ kPa]: (A) reactant conversions; (B) product selectivities; (C) selectivity of UOL isomers.

no effect is expected on the equilibrium conversion of the isomerization reaction, Eq. (2).

We investigated the effect of the feed reactant composition on the activity and product selectivities for HTR of MO with 2P on MgO by varying the 2P/MO ratio between 1.5 and 26. In Fig. 5, we have represented the evolution of reactant conversions and product selectivities as a function of the MO/(MO + 2P) molar ratio. Experiments were performed at 523 K, $W/F_{MO}^0 = 15$ g cat/h mol MO and $P_{2p}^0 = 6.6$ kPa (2P partial pressure in the feed). Thus, W/F_{2p}^0 and the MO partial pressure in the feed (P_{MO}^0) increased upon increasing MO/(MO + 2P) ratio.

Fig. 5A shows that X_{2P} increases monotonically from 3 to 36% by increasing the MO/(MO + 2P) ratio from 0.037 to 0.40, reflecting the simultaneous increase of W/F_{2p}^0. As predicted by thermodynamics and reaction stoichiometry, X_{MO} decreases with MO/(MO + 2P) ratio in spite that W/F_{MO}^0 was kept constant in these experiments.

The product distribution at different MO/(MO + 2P) ratios is shown in Fig. 5B. Total UOL selectivity increases with P_{MO}^0 reaching a value of 44% at MO/(MO + 2P) = 0.4. However, for MO/(MO + 2P) ≥ 0.3, selectivity to UOL levels off because MO present in high concentration in the reactant mixture and DMK formed from 2P give rise to AC compounds (mainly phorones) that affect the selectivity to HTR products. In fact, increasing formation of AC compounds occurs mainly at expenses of *i*-MO and MIBC. Because UOL selectivity increases but X_{MO} diminishes as MO/(MO + 2P) increases, UOL yield reaches a maximum at a MO/(MO + 2P) ratio of about 0.2, i.e., at a $P_{MO}^0 \approx 1.3$ kPa. An optimum reductant/oxidant ratio has also been reported by De Bruyn et al. [8] for the liquid-phase reduction of benzalacetone with variable amounts of cyclopentanol on Zr-MCM-41. Finally, Fig. 5B shows that MIBK is not obtained in significant amounts at any reactant ratio.

Fig. 5C shows the effect of the feed composition on the selectivity of unsaturated alcohol isomers. Selectivity to UOL_1, the unsaturated alcohol formed from MO, continuously increases with increasing P_{MO}^0 reaching a value of about 35% for MO/(MO + 2P) = 0.4. In contrast, selectivity to UOL_2, the unsaturated alcohol formed from *i*-MO, slightly decreases

with P_{MO}^0, probably because formation of *i*-MO decreases with MO/(MO + 2P) (Fig. 5B). As a result, the UOL_1/UOL_2 ratio increases with P_{MO}^0 and reaches a value of about 4 for MO/(MO + 2P) = 0.4.

3.5. Effect of the reaction temperature

The effect of the reaction temperature on the HTR of MO with 2P was investigated. The catalytic test at each reaction temperature was carried out using a fresh catalyst load and a reactant mixture with 2P/MO = 5 (molar ratio) at $W/F_{MO}^0 = 15$ g cat h/mol MO. Results obtained at zero time on stream are presented in Fig. 6.

As expected, reactant conversions increased with temperature (Fig. 6A). The X_{MO}/X_{2P} ratio decreased from 6.0 (473 K) to 3.7 (573 K) probably reflecting both, the increasing 2P dehydrogenation activity to DMK and the diminution of AC formation rate from MO (Fig. 6B).

Szollosi and Bartok [26] found an optimum reaction temperature for conversion of 2-butanone (a saturated ketone) by HTR with 2P on MgO. They attributed this behavior to the shift of the reaction pathway toward formation of poisonous compounds at higher temperatures. Kaspar et al. [15] found that 523 K is the optimum reaction temperature for maximum total UOL selectivity in the HTR of 4-hexen-3-one with 2P on MgO since at lower and higher temperatures side reactions are favored. Contrarily, in our study the positive effect of reaction temperature on reactant conversions is probably due to the fact that total HTR products ($UOL_1 + UOL_2 + MIBK + MIBC$) prevail at all temperatures compared with aldol condensation products (Fig. 6B).

Total UOL formation increased with temperature (Fig. 6B) reaching values of $S_{UOL} \cong 44\%$ and $\eta_{UOL} \cong 37\%$ at 573 K. The UOL selectivity increase with temperature occurred essentially at expenses of MIBC. In a previous paper [17], we discussed that the selectivity for the HTR of MO with 2P is essentially determined by the reactant adsorption modes on the catalyst surface sites. As depicted in Scheme 2, simultaneous reduction of C=C and C=O bonds of mesityl oxides (MO and *i*-MO) to MIBC competes with selective reduction
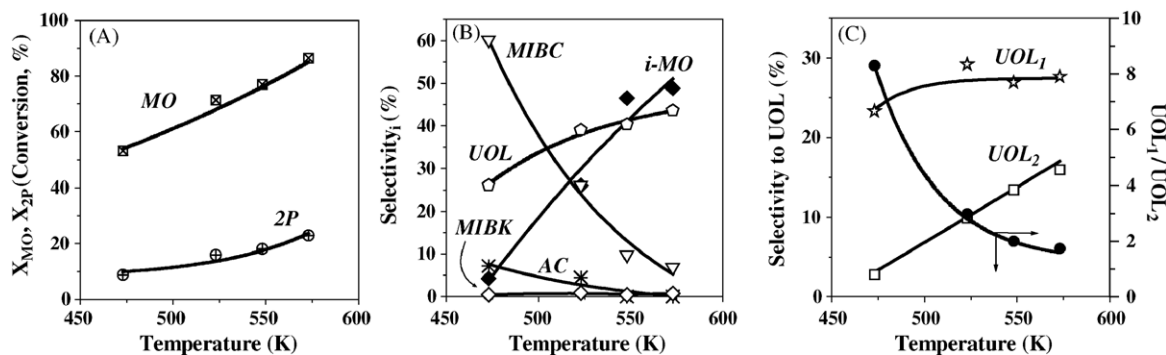
Fig. 6. Effect of reaction temperature on gas-phase HTR of MO with 2P [$P_T = 100$ kPa, $W/F_{MO}^0 = 15$ g h/mol MO, $N_2/2P/MO = 93.4/6.6/1.3$, kPa]: (A) reactant conversions; (B) product selectivities; (C) selectivity of UOL isomers.

of C=O bond of mesityl oxides to the corresponding allylic alcohols. Lewis acid Mg^{2+} cations such as those of MgO have been claimed to stabilize both, the quasi-planar di-π adsorption mode of C=C and C=O bonds and the di-$\sigma_{C=O}$ adsorption mode of C=O bond to about equal extent [27]. It seems from results of Fig. 6B that a reaction temperature increase is detrimental for the stability of the former adsorption mode and, thereby, decreases the concentration of surface reaction intermediates leading to MIBC.

Fig. 6B also shows that UOL can be obtained as the main reaction product at intermediate temperatures (specifically, at about 523 K), but *i*-MO is predominant at higher temperatures. Probably, the complex bimolecular transition state postulated for UOL formation (Scheme 1) is not stable enough at high reaction temperatures and the reaction pathway may then shift toward the simpler MO isomerization reaction that does not involve the hydrogen donor.

In Fig. 6C, we represented the selectivity evolution of UOL_1 and UOL_2 with temperature. It is observed that while S_{UOL1} increases slightly within the temperature range studied, the selectivity increase of UOL_2 is significant, from 3% (473 K) to 16% (573 K), which is consistent with its direct formation from *i*-MO. As a result, the UOL_1/UOL_2 molar ratio drops from 8.3 (473 K) to 1.7 (573 K), thereby showing that the allylic alcohol distribution may be controlled by temperature.

One of the most remarkable consequences of increasing the reaction temperature is the decrease of the catalyst deactivation rate, as it is inferred from Fig. 7 where we have plotted the evolution of MO conversion as a function of time on stream at different temperatures. In a previous work on MgO deactivation during aldol condensation reactions of acetone to MO and isophorone [28], we concluded that highly unsaturated C_9 compounds, such as phorone, formed by aldol condensation of MO with acetone remain strongly bound to the catalyst surface and block the active sites. Similarly, in the present reaction of MO with 2P, strong MO adsorption via the C=O bond on Mg^{2+} cations vicinal to strongly basic O^{2-} sites present on the catalyst surface, leads to formation of C_9 aldol condensation products (AC compounds) by aldol condensation reactions with acetone. Diminution of the MO sticking

coefficient with temperature would decrease the consecutive formation of C_9 coke intermediates via aldol condensation reactions, thereby decreasing the catalyst deactivation rate. This explanation is supported by results in Fig. 6B showing that the AC formation rate diminishes by increasing the temperature.

3.6. Effect of the hydrogen donor

The structure of the hydrogen donor may play a major role in HTR reactions since alcohol geometric and electronic properties affect the configuration of the transition state and, as a consequence, the product distribution. Thermodynamics of reaction (1) has to be taken into account also; for example, aliphatic secondary alcohols would have the best reducing capacities because the corresponding dialkyl ketones present the highest reduction potentials [6]. However, other factors such as the chemical structure of the reactant carbonyl compound may also define the nature of the reducing agent needed. For instance, bulky indanol is a much better hydrogen donor than aromatic 1-phenylethanol or aliphatic 2-propanol for the liquid-phase reduction of prostaglandin
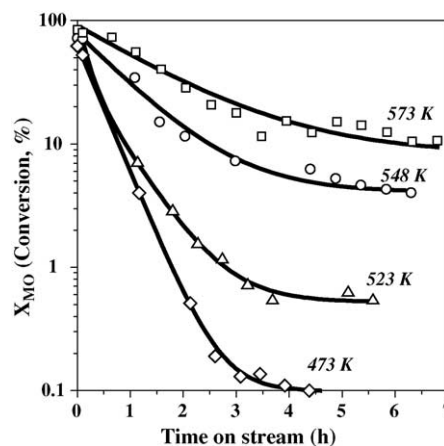

Fig. 7. Effect of reaction temperature on MgO deactivation during gas-phase HTR of MO with 2P [$P_T = 100$ kPa, $W/F_{MO}^0 = 15$ g h/mol MO, $N_2/2P/MO = 93.4/6.6/1.3$, kPa]. MO conversions as a function of time on stream.

Table 1
Effect of the hydrogen donor on the gas-phase HTR of mesityl oxide on MgO

Entry	Alcohol	Conversion[a] (%)		Selectivity[a] (%)				
		X_{MO}	$X_{Alcohol}$	UOL	i-MO	MIBC	MIBK	UOL_1/UOL_2
1	1-Propanol	35.3	5.7	34.4	57.6	6.6	1.4	1.9
2	2-Propanol	84.2	23.1	43.6	48.8	6.9	0.7	1.7
3	2-Butanol	88.0	27.2	40.7	54.6	3.4	1.3	1.5
4	1-Phenylethanol	73.1	14.9	38.9	55.7	4.8	0.6	2.0

$T = 573$ K; N$_2$/alcohol/MO = 93.4/6.6/1.3 kPa; $W/F_{MO}^0 = 15$ g h/mol.

[a] At $t = 0$.

precursor enones to unsaturated alcohols on MCM-41 [8]. In contrast, Corma et al. [9] showed that aliphatic 2-butanol is better than cyclopentanol or 1-phenylethanol for the liquid-phase reduction of cyclohexanone on Sn-MCM-41. Authors sustain that steric limitations at the Lewis active site and not related to pore size, make that the bulkier the hydrogen donor, the lower the activity.

Table 1 illustrates the catalytic performance of MgO for the HTR of MO when different alcohols are used as a hydrogen source. Comparison between aliphatic primary and secondary alcohols with the same carbon atom number (entries 1 and 2, respectively) shows that, as expected, secondary alcohols are better hydrogen donors since aldehydes have lower reduction potentials than dialkyl ketones of the same carbon atom number [6]. Primary 1-propanol conversion is lower than the expected for 100% selectivity of Eq. (1) and an alcohol/MO = 5 ratio in the feed. Therefore, not enough hydrogen can be transferred from 1-propanol to MO and the MO isomerization to i-MO prevails.

Increasing the carbon atom number of secondary alcohols does not affect significantly either the activity or total UOL selectivity (entries 2 and 3). Methyl ethyl ketone (product of 2-butanol oxidation) and acetone (product of 2-propanol oxidation) have similar reduction enthalpies [6] and consequently, the corresponding alcohols have comparable reducing properties. The slight differences in catalytic behavior using 2-propanol or 2-butanol are not attributable to steric limitations since MgO has a pore diameter of 30 Å, large enough to accommodate the resulting transition states in both cases.

A secondary aryl alcohol such as 1-phenylethanol (entry 4) gives a much lower conversion compared to 2-propanol, probably because acetophenone (the product of 1-phenylethanol oxidation) has a lower reduction potential compared with 2-propanol [6]. In addition to thermodynamics, geometrical and electronic properties have to be taken into account in this case since the aromatic ring may hinder formation of the transition state and probably competes with the alcoholic function for the coordination on the Lewis site [9].

4. Conclusions

Mesityl oxide isomers are efficiently reduced in gas phase by 2-propanol on MgO to the corresponding allylic alco-

hols. MgO contains weak acid-strong base Mg^{2+}–O^{2-} pair sites that promote formation of the 6-atom cyclic intermediate needed in Meerwein–Ponndorf–Verley mechanism for preferentially transferring hydrogen from 2-propanol to the C=O bond of mesityl oxide isomers. Main competitive reaction is the unselective reduction of mesityl oxide isomers to methyl isobutyl carbinol, the saturated alcohol, which requires participation of surface hydrogen fragments provided by dehydrogenation of 2-propanol to acetone.

Total allylic alcohol yield may be improved by optimizing the reaction operation conditions. Increasing the contact time increases both the mesityl oxide conversion and the yield to allylic alcohols, in particular to 4-methyl-3-penten-2ol. By changing the feed reactant composition at a given contact time, a maximum allylic alcohol yield is reached for a 2-propanol/mesityl oxide ratio close to 4. This is because the allylic alcohol selectivity diminishes whereas mesityl oxide conversion increases with increasing 2-propanol/mesityl oxide ratio. Low 2-propanol/mesityl oxide ratios favor formation of the 4-methyl-3-penten-2ol isomer directly from mesityl oxide. Temperature plays a major role on catalyst selectivity and stability. Formation of methyl isobutyl carbinol is drastically suppressed by increasing the temperature, probably because of the instability of surface intermediates involved in the reaction. As a consequence, the yield to allylic alcohols, in particular to 4-methyl-4-penten-2ol, increases with temperature. Since 4-methyl-3-penten-2ol formation was less sensitive to reaction temperature, 4-methyl-3-penten-2ol/4-methyl-4-penten-2ol ratios as high as 8.3 can be obtained at low reaction temperatures. On the other hand, the catalyst activity decay drastically diminishes by increasing the temperature because formation of C$_9$ coke intermediates from mesityl oxide via aldol condensation reactions is suppressed.

Total allylic alcohol yield is significantly higher when using 2-propanol than 1-propanol because secondary alcohols are better hydrogen donors. But the allylic alcohol formation rate is not changed when 2-propanol is replaced by heavier secondary alcohols, such as 2-butanol. In contrast, mesityl oxide conversion and allylic alcohol yield are lower when using 1-phenylethanol as compared to 2-propanol, probably because the aromatic ring of secondary aryl alcohols hampers formation of the intermediate transition state. The ratio of the two unsaturated alcohol isomers was almost not affected by the nature of the hydrogen donor.

Acknowledgments

References

[1] V. Ponec, Appl. Catal. A 149 (1997) 27.

[2] R.L. Augustine, Catal. Today 37 (1997) 419.

[3] M.G. Musolino, P. De Maio, A. Donato, R. Pierpaolo, J. Mol. Catal. A: Chem. 208 (2004) 219.

[4] M. von Arx, T. Mallat, A. Baiker, J. Mol. Catal. A: Chem. 148 (1999) 275.

[5] C. Milone, R. Ingoglia, A. Pistone, G. Neri, F. Frusteri, S. Galvagno, J. Catal. 222 (2004) 348.

[6] C.F. de Graauw, J.A. Peters, H. van Bekkum, J. Huskens, Synthesis (1994) 1007.

[7] G. Szollosi, M. Bartok, J. Mol. Catal. A: Chem. 148 (1999) 265.

[8] M. De Bruyn, M. Limbourg, J. Denayer, G.V. Baron, V. Parvulescu, P.J. Grobet, D.E. De Vos, P.A. Jacobs, Appl. Catal. A: Gen. 254 (2003) 189.

[9] A. Corma, M.E. Domine, S. Valencia, J. Catal. 215 (2003) 294.

[10] E.J. Creyghton, S.D. Ganeshie, R.S. Downing, H. van Bekkum, J. Mol. Catal. A: Chem. 115 (1997) 457.

[11] S.N. Coman, V.I. Parvulescu, M. De Bruyn, D.E. De Vos, P.A. Jacobs, J. Catal. 206 (2002) 218.

[12] Y. Zhu, G. Chuah, S. Jaenicke, J. Catal. 227 (2004) 1.

[13] K. Takagi, H. Izumida, M. Yamamoto, S. Anzai, Y. Ichihashi, S. Nishiyama, S. Tsuruya, in: Proceedings of the 13th International Congress on Catalysis, Paris, 2004, p. 263, P5-077.

[14] T.M. Jyothi, T. Raja, B.S. Rao, J. Mol. Catal. A: Chem. 168 (2001) 187.

[15] J. Kaspar, A. Trovarelli, F. Zamoner, E. Farnetti, M. Graziani, in: M. Guisnet, et al. (Eds.), Heterogeneous Catalysis and Fine Chemicals II, Elsevier Science, Amsterdam, 1991, p. 253.

[16] J. Kijenski, M. Glinski, J. Czarnecki, R. Derlacka, V. Jarzyna, in: M. Guisnet, et al. (Eds.), Heterogeneous Catalysis and Fine Chemicals III, Elsevier Science, Amsterdam, 1993, p. 631.

[17] J.I. Di Cosimo, A. Acosta, C.R. Apesteguía, J. Mol. Catal. A: Chem. 222 (2004) 87.

[18] J.I. Di Cosimo, V.K. Díez, C.R. Apesteguía, Appl. Catal. A 137 (1996) 149.

[19] V.K. Díez, C.R. Apesteguía, J.I. Di Cosimo, J. Catal. 215 (2003) 220.

[20] R. Philipp, K. Fujimoto, J. Phys. Chem. 96 (1992) 9035.

[21] H. Hattori, Appl. Catal. A 222 (2001) 247.

[22] A. Gervasini, A. Auroux, J. Catal. 131 (1991) 190.

[23] V.K. Díez, C.R. Apesteguía, J.I. Di Cosimo, Catal. Today 63 (2000) 53.

[24] I.M. Klotz, R.M. Rosenberg, Chemical Thermodynamics: Basic Theory and Methods, sixth ed., John Wiley and Sons, New York, 2000.

[25] S.R. de Miguel, M.C. Román-Martinez, D. Carzola-Amorós, E.L. Jablonski, O.A. Scelza, Catal. Today 66 (2001) 289.

[26] G. Szollosi, M. Bartok, Appl. Catal. A: Gen. 169 (1998) 263.

[27] F. Delbecq, P. Sautet, J. Catal. 152 (1995) 217.

[28] J.I. Di Cosimo, C.R. Apesteguía, J. Mol. Catal. 130 (1998) 179.